Using size distributions for determining growth mechanisms of grain boundary precipitates

Conference or Workshop Item

Using Size Distributions for Determining Growth Mechanisms of Grain Boundary Precipitates

Shirley Northover (née Payne)

Faculty of Mathematics, Computing and Technology, The Open University,
Walton Hall, Milton Keynes, MK7 6AA, United Kingdom

Keywords: size distribution, grain boundary precipitates, growth, coarsening, kinetics

Abstract

In the past various single parameters such as the mean, mode or maximum of the precipitate size distribution have been used in experiments to determine growth mechanisms. In the present study the development with aging time of the size and shape distributions of bcc precipitates at grain boundaries in an fcc material (Co-20Fe at 1003^{o}K) have been compared with possible theoretical models to determine the rate controlling process. The growth of these precipitates is initially well described by the grain boundary dependent collector plate mechanism of Brailsford and Aaron. As the precipitates grow low energy facets are formed which can move only by the propagation of ledges and growth becomes interface controlled. The precipitates' diffusion fields soon overlap and coarsening occurs with interface control. The results demonstrate that this would not have been revealed using simpler measures of precipitate size.

Introduction

The growth of grain boundary precipitates (GBPs) is important in determining the behaviour of many technologically important materials from the hardenability of steels to the corrosion resistance of light alloys.

There are long-standing models of diffusion controlled GBP growth and these have been developed to include both growth and coarsening in the same treatment (1). With advances in computing power there have been increasingly sophisticated simulations of grain boundary microstructural development but there remain relatively few experimental studies to compare with their results and these have usually measured the mean particle size eg.(2)(3)(4)

During GBP growth and coarsening both the development of the size distribution and the rate laws followed will depend on the underlying mechanisms and this paper describes measurements of GB bcc precipitates in an fcc matrix in an alloy that was originally used to model the behaviour of steels (5) to determine which mechanism is rate determining and to compare the results with various possible models for the growth of GBPs.

Experimental procedures

An alloy of composition Co-19.6$\pm$0.4wt%Fe, prepared by vacuum melting 99.999% purity Co and 99.999% purity Fe, was homogenised and rolled to thin strip. Pieces encapsulated in silica under an argon atmosphere were solution treated at 1200C for 30 minutes and aged at 730C for 0.25, 0.5, 1, 6, 24 or 113 hours followed by a water quench. The surface layers were removed and the specimens, mounted in conducting Bakelite, were polished to 1μm with diamond paste and then jet electropolished at 110V in a solution of 22ml perchloric acid, 118ml butan-1-ol, 390ml methanol at -45C to remove the damaged layer before examining in channelling contrast in an ISI 100A scanning electron microscope. A Quantimet 720 was used to measure the precipitates' lengths areas and aspect ratios (as reflected in the ratio of the maximum to the minimum of four feret diameters measured at 45° to each other) from tracings of the images of the two longer aged microstructures. On some samples the Quantimet could not distinguish

between the smallest precipitates and pits caused by etching and in these cases a scaled proportion of the size distribution of features within the grain which would, if at grain-boundaries, have been counted as precipitates was subtracted from the observed distribution before calculation of the true volume size distribution. The errors introduced in tracing and by the finite pixel size of the Quantimet proved significant for the smaller precipitates in the shorter aged specimens and the lengths of these were measured by hand.

Stereology, sectioning effects, data handling and representation of size distribution

The precipitates were roughly ellipsoidal and distributed along boundaries almost perpendicular to the specimen surface. To correct for the distortion of the size distribution by the greater volume sampled for larger precipitates by measurements made on a planar section, the particles were approximated to pairs of spherical caps lying on boundaries perpendicular to the specimen surface and uniformly distributed through the specimen thickness, and a modification of the Schwartz-Saltzykov approach (6) was used to extract the true size distribution.

The shape factor given by the maximum-minimum of 4 45° feret diameters depends not only on the aspect ratio of a precipitate but on its inclination to the axes of measurement and the maximum of 4 feret diameters measured at 45° to one another gives up to 8% underestimate of the maximum feret diameter This greatly distorts the observed distribution of aspect ratios and these effects were corrected for using standard stereological methods (7).

The resolution on the micrographs was better than 0.1μm. When using the Quantimet large prints were traced so this resolution was not degraded.

The procedure for deriving the true size distribution relies on an accurate initial assessment of the frequency of occurrence of the largest particles and errors in subsequent size classes are compounded. It is essential to have enough particles in the highest classes to ensure this sampling error is small and this requirement set a lower limit to the bin width and the total number of particles measured.

The initial hand sizing was carried out with a bin width close to 0.15μm and calculations were performed using bins $\sim$ 0.3μm wide. The automatic counting was done with a bin width of 0.5μm. The mean size of all members of a bin was taken as the median size of that bin.

In all cases where data was acquired by hand at least 700 measurements were made for each specimen and over 300 and 1200 particles were measured on the 24 hr and 113 hr aged material, respectively.

The use of cumulative frequency plots reduces the effects of sampling errors on the shape of the size distribution as these are random in each bin and will tend to average to zero overall but cumulative frequency plots are difficult to compare. A log / normal probability plot is a more convenient way of displaying the size distribution but the rapidly expanding scale of the plot at each end magnifies any inaccuracies at the lower end introduced in background subtraction or by accumulated stereological errors and at high end due to accumulated rounding errors.

Results

The results of the size measurements are summarised in Table 1 and representative cumulative frequency / size distributions are plotted on log-normal scales in fig. 1. The size distributions were all log normal up to 24hrs aging time. After 113 hrs ageing the precipitate size distribution was no longer unimodal, showing at least 3 peaks, possibly with smaller peaks above these. The distribution of aspect ratios of precipitates in 24 hr and 113 hr aged material are shown in fig. 2.

Although barely visible in the sizing by feret diameter, sizing the precipitate images by area showed that even at 24 hrs the precipitate size distribution departs from being unimodal.

Each of the 3 individual sets of data collected from images at different magnifications showed peaks and troughs in similar positions demonstrating this as a true feature of the area distribution

rather than an artifact of statistical fluctuations in the populations of each bin. This overall pattern was maintained in the areal distribution of the 113 hr aged material with a strong double peak followed by 3 subsidiary peaks, although the distribution was broader and, of course, shifted to larger sizes.

Table 1. Grain boundary precipitate sizes

Specimen ageing time	feret diameter (μm)			Precipitate diameter (μm)			
	mean	Geometric mean	mode	mean	Geometric mean	mode	max
15 min	0.77	0.66	0.55 ± 0.1	0.89	0.80	0.6 ± 1	2.25
30 min	1.03	0.93	0.8 ± 0.1	1.22	1.16	1.2 ± 0.1	2.33
60min	1.16	0.95	1.0 ± 0.2	1.34	1.13	1.2 ± 0.2	3.83
24 hr	2.99	2.63	2.1 ± 0.2	3.63	3.39	2.25 ± 0.2	8.0 or 11.75*
113 hr	4.87	4.2	3.75 or 5.25	6.01	5.48	3.75 or 5.25 or 6.75 **	12.25

* may be due to particle impingement ** three peaks in the distribution

(a) (b)

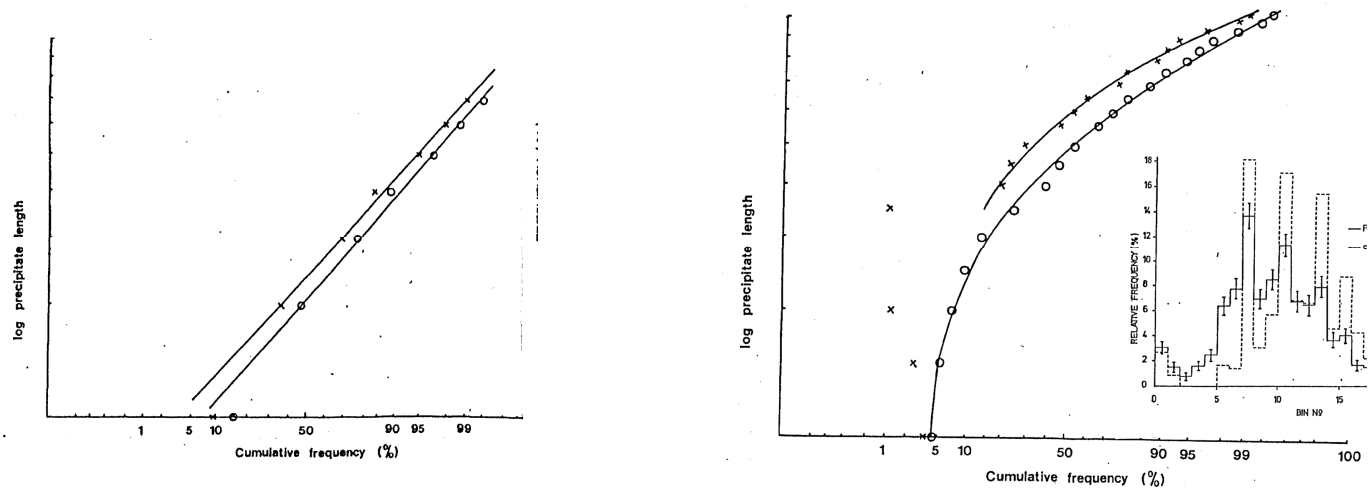

Figure 1 Cumulative frequency size distributions for a α precipitate at grain boundaries of Co-20Fe aged at 730°C for a)15' b) 113 hours

Discussion

Rate laws expected from different controlling mechanisms for growth

Growth of GBPs by different mechanisms will produce different size distributions and different rate laws during growth and coarsening. In general the precipitate size distribution will be broader for interfacial controlled than for diffusion controlled growth (8) and any interface control will reduce growth rates. Possible mechanisms and the rate laws and size distribution predicted for them are:

a) Volume diffusion:

During growth this will give $\ell \alpha t^{1/2}$ but if growth in 1 dimension is inhibited $\ell \alpha t$ (9). During coarsening $\ell \alpha t^{3/2}$ (or $\ell \alpha t^3$ if there is inhibited thickening) and the size distribution will show a sharp cut-off (10) at $\ell_{max} = 1.5\ \bar{\ell}$ ($\bar{\ell}$ is the size precipitate which is neither growing nor shrinking).

b) Collector Plate Mechanism

According to the treatment of Aaron and Aaronson (11) $\ell \alpha t^{1/4}$ or following that of Brailsford and Aaron (12) $\ell \alpha t^P$, $1/4 < P < 0.37$. In the presence of inhibited thickening this would again give a rate law $\ell \alpha t^{1/2}$.

c) Interface control by rate of diffusion around precipitate / matrix interface during growth

$\ell \alpha t^{1/2}$ but coarsening $\ell_{max} = 2\ \bar{\ell}$

d) Interface control by inhibition thickening (eg. ledge mechanism)

$\ell \alpha t^{1/2}$ and during coarsening $\ell_{max} = 2\bar{\ell}$

Precipitate lengths

Apart from the overall increase in precipitate size, the precipitate size distributions showed no obvious systematic variation up to 24 hrs of ageing but after 113 hrs ageing the precipitate size distribution was no longer unimodal, showing at least 3 peaks (the smaller peaks above these may possibly be due to impingement of GBPs individually belonging to the size classes of these 3 peaks). Some of this splitting may be due to the formation of cellular colonies, the growth of which was seen to be just starting after 24 hrs aging and which were well developed after 113 hrs. The earlier onset of coarsening in some boundaries than others would also lead to a splitting such as that observed in this case; instead of a steady shift of the distribution from that typical of growth to that of coarsening, several different stages of the transition would be superimposed. Coarsening will occur sooner in a boundary where precipitate densities are high, diffusion along the boundary is particularly fast or the precipitates are of a particularly fast growing habit since these factors will all lead to an early overlapping of diffusion fields.

Precipitate sizing by image area

Even at 24 hrs the precipitate area distribution departs from being unimodal supporting the onset of coarsening at some boundaries prior to 24 hrs ageing. Areal sizing will also pick up effects due to differing degrees of inhibition of thickening at different boundaries, which will have only an indirect effect on the measurements of precipitate length. This overall pattern continued in the areal distribution of the 113 hr aged material with a strong double peak followed by 3 subsidiary peaks which may be due to impingement of precipitates with areas corresponding to the strong peaks. The number of bins used for areal sizing was not large enough to show the upper limit of the 113 hrs size distribution but the general shape of the distributions is clearly different from that after 24hrs.. The envelope of the 24 hr distribution is a typical growth size distribution, skewed to the left, and the 113 hr tends to skew to the right, as for coarsening.

Aspect ratios

The distribution of aspect rations of the precipitates as in Fig. 2 shows a suggestion of a double peak in the 24 hr aged material. The approximate method used to evaluate the shape factor does not allow resolution of the fine structure of the distribution but it is clear that as aging has progressed the aspect ratio distribution has narrowed slightly and the mean particle shape has shifted towards a more elongated form. This shows inhibited thickening of precipitates as they grow. TEM and microanalysis around the precipitates (13) confirmed that formation of low energy facets is favoured so that further growth can occur only by a ledge mechanism. The development of cellular colonies, whose formation and growth will give a peak superimposed on the distribution for grain boundary allotriomorphs and moving gradually towards the lower $^{\omega}/\ell$ end of the distribution as growth of the colony proceeds, will also contribute to the observed peak shift.

Choice of parameters to characterise distributions

In studies of growth, nucleation often continues during the time of observation and the size distribution arises from precipitates nucleated over a range of time. In such cases the largest observed precipitate is conventionally assumed to have nucleated first and its growth kinetics are taken to be typical of all precipitates in the population eg (14) This seems inherently unlikely as the largest precipitates, if nucleated first, are those in particularly favourable sites, so their growth kinetics are likely to differ from those of gbps nucleated in more general higher energy sites. In the case of Co-20Fe the average number density of precipitates, although varying strongly from boundary to boundary, was found to change little with aging time, suggesting that,

once nucleated, the precipitates rapidly depleted the surrounding boundary of solute, so inhibiting further nucleation.
Compositional measurements (13) have shown that in the longer aged specimens the diffusional fields of the precipitates overlap in the boundary but not in the matrix, so coarsening was occurring between the grain boundary precipitates, while simultaneously solute was being provided by volume diffusion from the bulk, either directly or via the g.b., giving further growth and an increase in the GBP volume fraction.
To test the validity of the usual measurements on large precipitates, the variation with time of 3 different measures of the precipitate size distribution; the arithmetic mean size, the geometric mean, the mode (which for a log-normal distribution should equal the geometric mean) and the size of the largest precipitates, were compared. The results are shown in table 2. The incubation time for the onset of nucleation is unknown so results were calculated for both 0 and 600s incubation times.

Table 2 Growth rates calculated from single parameters derived from the size distribution

Aging time	Arithmetic mean ppt length (μm)	Growth rate ($m\ s^{-1}$) Zero Incubation Time		Growth rate ($m\ s^{-1}$) 600s Incubation Time	
		Population mean	Largest precipitates	Population mean	Largest precipitate
15 min	0.89	3.22×10^{-10}	1.51×10^{-9}	$7.48\ 10^{-10}$	2.94×10^{-9}
30 min	1.22	1.98×10^{-10}	8.80×10^{-10}	2.64×10^{-10}	1.37×10^{-9}
60min	1.34	1.22×10^{-10}	6.71×10^{-10}	1.33×10^{-10}	8.29×10^{-10}
24 hr	3.63	1.32×10^{-11}		1.08×10^{-11}	
113 hr	6.01	4.48×10^{-12}		3.36×10^{-12}	

The arithmetic & geometric mean sizes increase steadily with time giving $n \simeq 0.3$ assuming zero incubation time and $n \simeq 0.26$ for an incubation time of 600s. This agrees with the value of n = ¼ predicted by the simple collector plate mechanism of Aaron and Aaronson (11) or $¼ \leq n \leq 0.37$ given by Brailsford and Aaron's treatment (12). The mode sizes behave rather erratically (presumably as a result of the complicated interplay of continued growth and overlap of the precipitates' boundary diffusion fields) but the largest precipitates show a different behaviour from that of the means. Initially the maximum precipitate size increases more rapidly than the mean with n = 0.45 for 0 incubation time or n = 0.61 for 10 min incubation time but later increases more slowly with $n \simeq 0.22$. This behaviour reflects the change over from predominant growth to coarsening of the precipitates. Initially the precipitate sizes follow a log-normal distribution. When growth has almost ceased and coarsening dominates the size distribution developed increases with increasing size and has a sharp cut off at a small multiple of the size of the precipitate which is neither growing nor dissolving ($\bar{\ell}$). This cut off is at $\ell_{max} = 1.5\ \bar{\ell}$ for diffusion controlled coarsening & $\ell_{max} = 2.0\ \bar{\ell}$ for interface controlled coarsening. For the 113 hr aged material the largest precipitates were 12-13μm long, the arithmetic mean size being 6.0μm and the geometric mean 6.7μm. The distribution had several subsidiary peaks but was in general roughly of the shape indicated by the dashed curve of Fig. 3. $\ell_{max} \sim 2.0\ \bar{\ell}$ which indicated interface controlled coarsening.
If during growth $\ell = kt^n$; $\frac{d\ell}{dt} = nkt^{n-1} = \frac{n\ell}{t}$ and the largest precipitates will grow faster than those of mean size even when growing by the same mechanism.

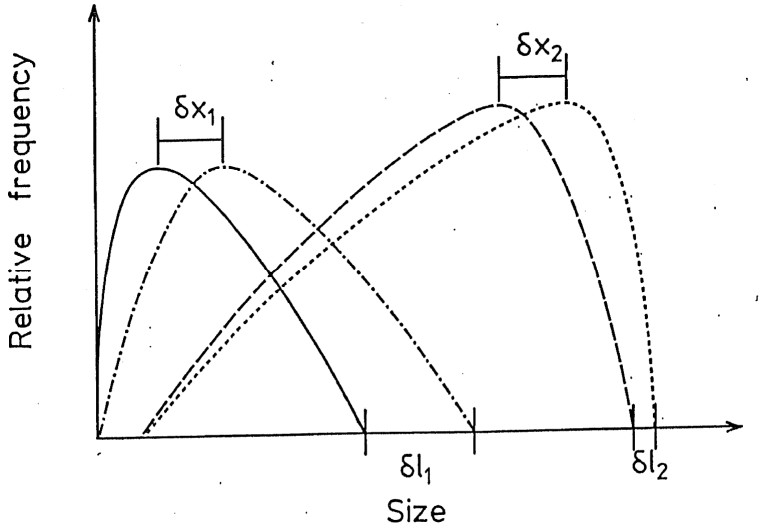

Fig.3 Development of size distribution during aging.

In the coarsening regime, however, the precipitate size distribution will be developing from that of solid line in Fig. 3 to that shown by the dotted line. During growth the distribution will change from that of the solid curve, through that of the dashed and dotted curve so that $d\ell_1 / dt > dx_1 / dt$. Later as coarsening proceeds and the distribution develops a sharper cut off the distribution will change from that shown by the dashed curve to that of the dotted curve so $dx_2 / dt > d\ell_2 / dt$. This agrees with the observed behaviour with $\frac{d\ell max}{dt}$ being initially greater than $\frac{d\bar{\ell}}{dt}$, but decreasing faster as ageing proceeds.

Determination of growth mechanism

The n value of ½ observed for the growth of the largest precipitates cannot be due to pure volume diffusion control because lengthening of these is obviously faster than that of small precipitates growing by a collector plate mechanism. This value of n = ½ must therefore be due to interface control. The largest precipitates are observed to be long and narrow, lying along the boundary so the most probable growth mechanism is interface control via inhibition of thickening (rather than rate of diffusion around the precipitate / matrix interface being limiting). If solute is supplied by the collector plate mechanism and is rapidly distributed around the precipitate but growth in one dimension is limited by the presence of a low energy facet, instead of $\ell \propto t^{1/4}$, the other dimensions of the precipitate will vary as $t^{1/2}$ - as observed. The formation of such a facet will be favoured if a low energy interface lies close to the boundary plane – giving a thin precipitate along the boundary. A STEM study of the diffusion fields around the precipitates confirmed this growth inhibition (13)

Comparison with model of Aaron and Aaronson (11)

The theory of Aaron and Aaronson (11) gives

$$\frac{d\ell}{dt} = \frac{2A_V D_V^{1/2}(C_\gamma^{Fe} - C_\gamma^{Fe})}{\pi 3/2(C_\alpha^{Fe} - C_{\alpha\gamma}^{Fe})\bar{s}\ell t^{1/2}}$$ where $\bar{s}$ is the equivalent half thickness of the precipitate. The mean precipitate spacing along boundaries in a 900s aged specimen was 6.6μm so taking $A_v = 3 \times 10^{-11}$ and $D_v = 8.7 \times 10^{-19}$ and substituting the arithmetic mean values of the precipitate length for each ageing time gives the results shown in Table3. Comparison of Tables 2 and 3 shows reasonable agreement, the predicted growth rates being of the right magnitude, but good

agreement requires $\bar{s}$ to be larger than suggested by the observed aspect ratios ($^{\omega}/\ell \simeq 0.4$) for the shorter aged specimens and $\bar{s}$ smaller than observation would suggest for the longer aged specimens. This indicates that the disagreement between the two is due to more than an error in one of the approximations made and the discrepancy probably reflects the increasing contribution of coarsening.

Table 3 Results using the model of Aaron and Aaronson (11)

Aging time	Arithmetic mean ppt length (μm)	$\frac{\bar{s}}{(\mu m)}$	$\frac{\bar{s}}{\ell}$	$\frac{d\ell}{dt}$ for 0 incubation time (m s^{-1})	$\frac{d\ell}{dt}$ for 10 minutes incubation time (m s^{-1})
15mins	0.89	0.2	0.22	4.76×10^{-9}	8.27×10^{-9}
15mins	0.89	0.3	0.34	3.18×10^{-9}	5.50×10^{-9}
30mins	1.22	0.2	0.16	5.6×10^{-10}	7.0×10^{-10}
30mins	1.22	0.3	0.25	3.8×10^{-10}	4.6×10^{-10}
60mins	1.34	0.2	0.15	3.6×10^{-10}	3.8×10^{-10}
60mins	1.34	0.3	0.22	2.4×10^{-10}	2.6×10^{-10}
24hr	3.63	0.4	0.11	1.3×10^{-11}	1.3×10^{-11}
24hr	3.63	0.7	0.19	7.6×10^{-12}	7.6×10^{-12}
113hr	6.01	0.4	0.07	3.8×10^{-12}	3.8×10^{-12}
113hr	6.01	0.7	0.11	2.2×10^{-12}	2.2×10^{-12}
113hr	6.01	1.2	0.20	1.3×10^{-12}	1.3×10^{-12}

Comparison with model of Brailsford and Aaron (12)

The theory of Brailsford and Aaron (12) gives the flux to the growing precipitate as

$$J = \frac{2D_b(C_\gamma^{Fe} - C_{\alpha\gamma}^{Fe})}{\ell[\ell n\frac{(2D_b^{\sigma})}{\ell D_V} + 0.116]}$$

If the precipitate shape is modelled as approximating to a growing disc of radius $\ell/2$ and thickness t^1, with a geometric factor Z of order unity to allow for the difference between this shape and the true one, the growth rate will be given by:

$$Z \times 2\pi \frac{\ell}{2} t^1 \times \frac{1}{2} \frac{d\ell}{dt} = \frac{\pi \ell \delta J}{C_{\alpha\gamma}^{Fe} - C_\alpha^{Fe}}$$

Using a value of $D_b = 9 \times 10^{-13}$ $m^2 s^{-1}$ and taking $t^1 \approx 0.35\ell$, Z = 1 and substituting into the equation.

$$\frac{d\ell}{dt} = \frac{4D_b\delta(C_\gamma - C_{\alpha\gamma})}{Z\ell t^1[\ell n(\frac{2D_b\delta}{\ell D_V}) + 0.116](C_{\alpha\gamma} - C_\alpha)}$$ gives the results shown in Table4.

Table 4 Growth rates from the model of Brailsford and Aaron (12)

Ageing time	Arithmetic mean precipitate length (μm)	T^1 (μm)	$d\ell/dt$ (m s^{-1})
15mins	0.89	0.3	5.50×10^{-10}
30mins	1.22	0.45	2.79×10^{-10}
1hr	1.34	0.48	2.42×10^{-10}
24hr	3.63	1.25	4.0×10^{-11}
113hr	6.01	2.2	1.5×10^{-11}

Comparing Table 2 and 4, gives the values of Z necessary for exact agreement shown in Table 5

Table 5 Required value of Z for exact agreement with model of Brailsford and Aaron (12)

Ageing time	Z for 0 incubation time	Z for 600s incubation time
15mins	0.6	1.36
30mins	0.7	0.95
1hr	0.5	0.55
24hr	0.33	0.27
113hr	0.30	0.22

The necessary values of Z are all close to 1 showing the good agreement between the Brailsford and Aaron treatment and the observed growth behaviour. The apparent decrease of Z with ageing time is another indication of the inhibition of thickening as growth proceeds. As the precipitate grows the apparent value of Z should increase if shape is preserved since $\frac{dv}{dt} = \frac{3d\ell}{dt}$ in this case. As Z decreases with ageing time $\frac{dv}{dt}$ is obviously increasing less fast than $\frac{d\ell}{dt}$ so thickening must be much slower than lengthening.

Effects of boundary structure on growth rates

The improved agreement of the Brailsford and Aaron treatment as compared to the Aaron & Aaronson treatment indicates that boundary diffusivity is not infinitely fast compared to volume diffusion, so that variations in boundary structure which affect the grain boundary diffusion coefficient will directly affect the growth precipitates. This effect of structure on growth will be in addition to the indirect effects through the orientation relationship between the precipitate and the neighbouring grains which will be determined initially by the structure at the nucleation site.

Conclusions

The rate of growth of the grain boundary α allotriomorphs of mean size in Co-20Fe aged at 730°C is initially well described by the Brailsford and Aaron treatment of the boundary diffusivity dependent collector plate mechanism. As the precipitate size increases inhibition of thickening leads to interface controlled growth and coarsening occurs with interface control. The largest precipitates are long and narrow with a low energy interface lying close to the boundary plane. In these GBPs inhibition of thickening occurs right from the start of growth, giving different growth behaviour from that of the majority of the precipitate population as the largest precipitates' growth is interface controlled from earliest times. This shows the importance of studying the development of the overall size distribution in experimental studies to determine growth mechanisms and kinetics.

References

1) Jiang, H., Faulkner, R.G. Acta Mat. 44 (1996)1857
2) Fujii,T., Moriyama, M., Kato, M., Mori, T. Phil. Mag. A68 (1993) 137
3) Jiang, H., Faulkner, R.G. Acta Mat. 44 (1996) 1865
4) Monzen, R., Hasegawa, T. Phil. Mag. Lett. 76 (1997) 69
5) Ryder, P.L., Pitsch, W. Acta Met.14 (1966) 1437
6) Saltykov, S.A. 'Stereometric Metallography', Metallurgizdat, Moscow (1958)
7) DeHoff, R.T, Rhines, F.N. 'Quantitative Metallography'(1968)
8) Koiwa, M., Phil. Mag. 30 (1974) 877, 895
9) Horvay, G. Cahn, J.W. Acta Met. 9 (1961) 695
10) Kirchner, H.O.K. Met. Trans. 2 (1971) 2861
11) Aaron, H.B., Aaronson, H.I. Acta Met. 16 (1968) 789
12) Brailsford, A.D., Aaron, H.B. J.Appl. Phys. 40 (1969) 1702
13) Payne, S.M. PhD Thesis, University of Cambridge (1982)
14) De Hass, M,. De Hosson, J.T.M. Scripta Mat.44 (2001) 281